

Exact Cavity Perturbation Technique to Determine Complex Permittivity of Dielectric Materials

Charles H. Starr

Jet Propulsion Laboratory

Major: Applied Physics

USRP Summer Session

Date: 15 August 2011

Exact Cavity Perturbation Technique to Determine Complex Permittivity of Dielectric Materials

Charles H. Starr
Columbia University, New York, NY, 10027

and

Martin B. Barmatz
Jet Propulsion Laboratory, California Institute of Technology, Pasadena, CA, 91109

I. Introduction

A. Relevance to *Cassini*

Cassini is an international spacecraft mission facilitated by NASA and ESA which seeks to understand the Saturn planetary system, including rings and moons.¹ Launched in 1997, the *Cassini* spacecraft contains two major components: the *Cassini* orbiter that has been orbiting Saturn since October 2004, and the European-built *Huygens* probe that landed on Titan's surface in December 2004 to study its geology and atmosphere. Titan, Saturn's largest moon and the second largest moon in the solar system, possesses surface and atmospheric features similar to those of Earth, including lakes, seas, and mountains. A physical characterization of these features is critical to understanding the origin and evolution of Titan, whose surface composition reflects its geological history. Because Titan's atmosphere is largely composed of methane, it is believed that surface lakes are filled with mixtures of liquid hydrocarbons.

The *Cassini* orbiter's RADAR instrument has been scanning Titan's surface at the atmosphere-penetrating microwave frequency of 13.8 GHz since 2004. However, accurate interpretation of these data is limited by a lack of knowledge regarding dielectric properties of liquid hydrocarbons at cryogenic temperatures.² Therefore, it is of specific interest to experimentally determine values for the complex permittivities of various liquid hydrocarbon mixtures at the surface conditions of Titan. In particular, more accurate values for complex permittivity would improve estimates of lake depth and surface composition obtained from the instrument's altimetry and backscatter modes.

B. Conventional and Extended Cavity Perturbation

Though many techniques have been developed to measure complex dielectric constants, cavity perturbation has been one of the most popular and successful methods to study low-loss materials. To perform cavity perturbation, a sample of precise dimensions is inserted into a microwave resonant cavity, and the complex dielectric constant is computed based on shifts in the measured cavity resonant frequency and the measured cavity quality factor. In this paper, conventional cavity perturbation refers to a first-order theory developed for a cylindrical resonant cavity loaded with a low-loss sample limited to no greater than ~2% of the total cavity volume. This theory assumes that insertion of the sample does not disturb empty cavity fields, which allows loaded cavity fields to be approximated by empty cavity fields for small sample sizes. Extended cavity perturbation was initially developed to study the dielectric properties of fragile materials that cannot be prepared into cylindrical rods thin enough for the conventional method.³ Using cavity field expressions obtained by solving Maxwell's equations with appropriate boundary conditions at the cavity walls and at the sample-vacuum interface, extended cavity perturbation allows cylindrical samples of arbitrary size. Both methods are limited to two-region cylindrical cavities, though analogous techniques do exist for rectangular cavities.

C. Exact Cavity Perturbation

In this paper, we summarize a new patent-pending approach to computing complex dielectric constants of non-magnetic materials given certain resonant frequency and quality factor measurements.² Exact cavity perturbation uses equations first derived by Spicopoulos et al, which compute a theoretical complex resonant frequency of a cylindrical cavity containing an arbitrary number of radially-stratified regions (II.A).⁴ A theoretical total cavity quality factor is computed based on empty cavity resonant frequency and quality factor measurements, which estimate losses in the cavity walls and end plates (II.B). Because the cavity can contain numerous regions, each of

different electromagnetic properties, liquid samples contained within a holder of known permittivity and permeability can be studied. This technique also determines electromagnetic field configurations within the cavity and at the cavity wall with a sample inserted in the cavity. This has direct application to *Cassini* science objectives that require the dielectric constants of liquid hydrocarbon mixtures. Unlike the conventional and extended methods, which involve direct calculations of the real and imaginary parts of the complex dielectric constant, our implementation of exact cavity perturbation relies on an efficient numerical root-finding method (III).

II. Overview of Theoretical Computations

A. Theoretical Complex Resonant Frequency Computation

The theoretical complex resonant frequency is computed as a function of cavity parameters, each region's electromagnetic properties, and three non-negative integers that describe the normal mode of interest. The first number, l , represents the number of tangential full periods. The second number, m , represents the number of radial half periods. The third number, n , represents the number of axial half periods. A theoretical complex frequency f is defined as:

$$f = f' - i \cdot f''$$

$$f'' = f' / (2Q_c),$$

where Q_c is the theoretical quality factor of the entire cavity. Thus, the imaginary part of a complex frequency simply describes the cavity's quality factor.

As a simple example, the TM_{lmn} (transverse magnetic) mode has the following theoretical resonant frequency for a cavity completely filled (i.e. only 1 region) with a dielectric material:

$$f'_{theoretical} = \frac{c}{2\sqrt{\epsilon_r'}} \sqrt{\left(\frac{x_{l,m}}{\pi \cdot R}\right)^2 + \left(\frac{n}{h}\right)^2},$$

where ϵ_r' is the real part of the complex permittivity of the dielectric material, $x_{l,m}$ is the m^{th} root of $J_l(x) = 0$ (Bessel function of the first kind of order l), R is the internal cavity radius, and h is the cavity height.⁵ Q_c can be calculated using expressions for the electric and magnetic fields inside the cavity and knowledge of the surface resistance of the cavity walls.

To describe the method for computing the theoretical complex resonant frequency of a cylindrical cavity with numerous regions of differing dielectric properties, we use notation introduced in a summary of Sphicopoulos et al., written by Jackson⁶. To calculate the theoretical complex resonant frequency, Jackson defines a fourth-order matrix S (omitted for brevity) that is a function of cavity parameters, each region's electromagnetic properties, and the mode numbers l and n . The theoretical complex resonant frequencies correspond to the roots of the equation:

$$\text{Det } S = 0,$$

where Det is the determinant operator. The theoretical complex resonant frequency of an lmn mode corresponds to the m^{th} positive real root of the equation. In our implementation of this computation, we numerically solve this determinant equation using a built-in root-finder. We specify the mode number m by providing the root-finder with a complex frequency guess whose real part is sufficiently close to the m^{th} real root.

The imaginary part of the complex frequency obtained through this computation, however, only represents the quality factor due to losses in the dielectric sample. The following section will describe how the imaginary part of this theoretical complex resonant frequency is adjusted to include losses in the cavity wall.

B. Adjustment of Theoretical Complex Resonant Frequency to Include Wall Losses⁷

Because the theoretical complex resonant frequency obtained in II.A includes only electromagnetic losses within the dielectric sample, the imaginary part of this complex frequency must be manually adjusted to include wall losses. This is achieved using the following expression for the theoretical quality factor due to wall losses:

$$Q_{wall} = \frac{\omega_0 W_c}{P_{cylinder} + P_{endplate}},$$

where ω_0 is the measured empty cavity angular resonant frequency, W_c is the time-averaged total energy stored within the cavity's electric and magnetic fields, $P_{cylinder}$ is the power absorption in the conducting walls, and $P_{endplate}$ is the power absorption in the conducting end plates. W_c (omitted for brevity) is a function of the dielectric properties of each region, which allow electric and magnetic field values to be computed. $P_{cylinder}$ is a function of the

tangential component of the magnetic field, H_{\tan} , at the cavity walls and of the wall's frequency-dependent surface resistance R_s . P_{endplate} is a function of the time-averaged total energy stored within the cavity's magnetic fields and also of R_s . P_{cylinder} , P_{endplate} , and R_s are given below, though H_{\tan} and W_{magnetic} are omitted for brevity:

$$P_{\text{cylinder}} = \frac{R_s}{2} \iint_{\text{wall}} |H_{\tan}|^2 dS$$

$$P_{\text{endplate}} = \frac{4R_s}{h \cdot \mu_0} W_{\text{magnetic}}$$

$$R_s = \frac{\pi \cdot \mu_0}{Q_0} \frac{R \cdot h}{h + R} \sqrt{f'_{\text{theoretical}} \cdot f_0},$$

where f_0 and Q_0 are the measured empty cavity resonant frequency and quality factor, respectively. Then, the total cavity quality factor adjusted for wall losses is given as:

$$Q_c^{\text{total}} = \left(\frac{1}{Q_{\text{sample}}} + \frac{1}{Q_{\text{wall}}} \right)^{-1},$$

where Q_{sample} is the quality factor that corresponds to the imaginary part of the root of equation $\text{Det } S = 0$. With this adjusted quality factor, we define a new theoretical complex resonant frequency that will be used in further calculations:

$$f_{\text{theoretical}} = f'_{\text{theoretical}} - i \cdot f''_{\text{theoretical}} = f'_{\text{theoretical}} - i \cdot \frac{f'_{\text{theoretical}}}{(2Q_c^{\text{total}})}.$$

III. Numerical Determination of Complex Permittivity

The procedure described in this section strategically searches through the complex permittivity plane until a value is found that produces an $f_{\text{theoretical}}$ identical to f_{measured} , defined below:

$$f_{\text{measured}} = f'_{\text{measured}} - i \cdot \frac{f'_{\text{measured}}}{2Q_{\text{measured}}},$$

where f'_{measured} and Q_{measured} are experimental values for resonant frequency and total cavity quality factor. The complex permittivity plane is the set of all ordered pairs $(\epsilon_s', \epsilon_s'')$, for which ϵ_s' and ϵ_s'' represent the real and imaginary parts of the unknown dielectric constant of the sample region. It works to this method's advantage that ϵ_s' is strongly coupled to f_c but weakly coupled to Q_c^{total} while the reverse is true for ϵ_s'' . This simplifies computations because, in effect, the complex function

$$f_{\text{theoretical}}(\epsilon_s', \epsilon_s'') = f'_{\text{theoretical}}(\epsilon_s', \epsilon_s'') - i \cdot f''_{\text{theoretical}}(\epsilon_s', \epsilon_s'')$$

can be rewritten as

$$f_{\text{theoretical}}(\epsilon_s', \epsilon_s'') = f'_{\text{theoretical}}(\epsilon_s') - i \cdot \frac{f'_{\text{theoretical}}(\epsilon_s')}{Q_c^{\text{total}}(\epsilon_s'')}.$$

The procedure described below for numerically determining the sample's complex permittivity is divided into two steps. The first step returns a rough guess for the complex permittivity, which is fed into the second step, a complex root-finding algorithm that refines this guess to arbitrary accuracy.

A. An Initial Guess for Complex Permittivity

To obtain an initial guess for the complex permittivity, a grid corresponding to a finite range of complex permittivity values is defined in the complex plane. The horizontal (real) axis is defined by the closed interval $[\epsilon_s'_{\text{min}}, \epsilon_s'_{\text{max}}]$, which is divided into discrete steps of width $\Delta\epsilon_s'$. The vertical (imaginary) axis is defined by the close interval $[\epsilon_s''_{\text{min}}, \epsilon_s''_{\text{max}}]$, which is divided into discrete steps of width $\Delta\epsilon_s''$. Each iteration of this procedure is characterized by a complex permittivity $\epsilon_s = \epsilon_s' + i \cdot \epsilon_s''$ for which certain theoretical values will be evaluated.

Because f_c depends primarily on ϵ_s' and Q_c^{total} depends primarily on ϵ_s'' , the first stage of iterations will consist of incrementing ϵ_s' , with ϵ_s'' held fixed at an arbitrary but reasonable value until f_c is sufficiently close to f'_{measured} . For each iteration, $f'_{\text{theoretical}}$ is evaluated and compared to f'_{measured} . If, in incrementing ϵ_s' , $f'_{\text{theoretical}}$ crosses f'_{measured} , ϵ_s' is decremented once and the increment is halved to provide greater resolution. This is repeated until an ϵ_s' is

encountered that produces an $f'_{theoretical}$ equivalent to $f'_{measured}$, choosing an accuracy of at worst 1 part in 10^6 . This ϵ_s' will be used as the real part of the initial guess for the root-finding algorithm described in III.B.

An identical procedure is then performed for ϵ_s'' (with ϵ_s' held fixed at the initial guess just obtained), except during each iteration, Q_c^{total} (instead of $f'_{theoretical}$) is evaluated and compared to $Q_{measured}$. The imaginary part of the initial guess for ϵ_s'' is the first value which produces a Q_c^{total} equivalent to $Q_{measured}$, again choosing an accuracy of at worst 1 part in 10^6 .

B. Root-Finder to Determine Final Complex Permittivity

An initial guess for complex permittivity has been determined by requiring that the theoretical resonant frequency and quality factor corresponding to this initial guess be within 1 part in 10^6 of analogous measured quantities. However, more accuracy is required because complex permittivity is very sensitive to measurable shifts in resonant frequency and quality factor. For convenience, we define a complex function

$$G(\epsilon_s) = f_{measured} - f_{theoretical}$$

whose zero precisely corresponds to the permittivity of the sample. Because we will be solving the relation $G = 0$ numerically, certain real and imaginary null criteria (which are more strict than those imposed for the initial guess computation) will be specified. Like the initial guess computation, this solving algorithm treats the complex function $f_{theoretical}$ as two single variable real functions, but attempts to minimize G by varying ϵ_s' and ϵ_s'' simultaneously.

First, a rectangle is constructed in the complex permittivity plane, centered on the initial guess $(\epsilon_s'_{guess}, \epsilon_s''_{guess})$ from III.A. Initially, the dimensions of the rectangle are defined such that width is 1% of $\epsilon_s'_{guess}$ and the height is 1% of $\epsilon_s''_{guess}$. For subsequent iterations, however, the dimensions of the rectangle may be a different percentage of the center point value.

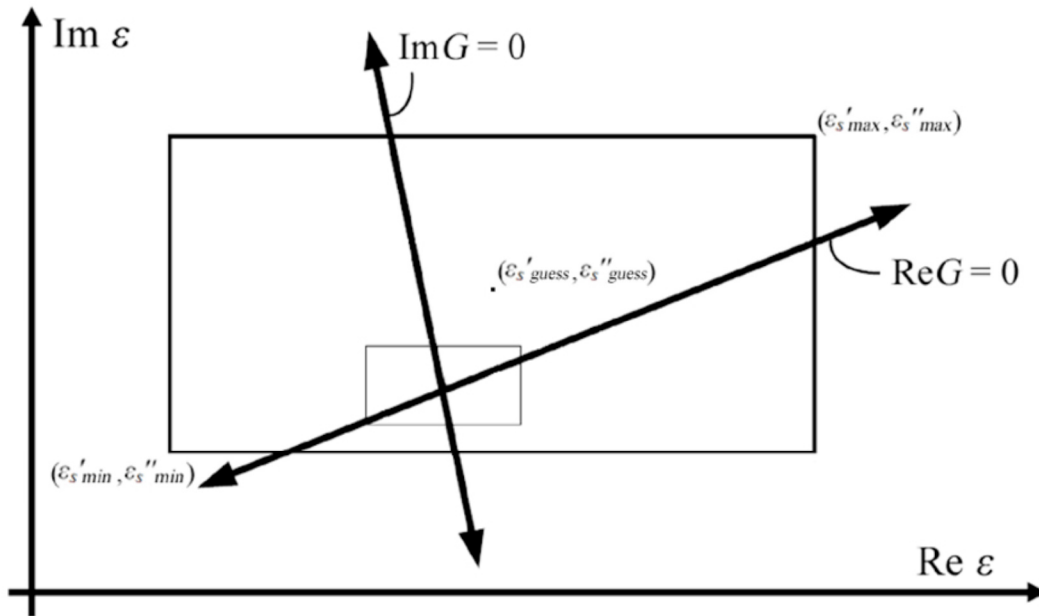


Figure 1. Visualization of Complex Root-Finding Algorithm

The goal of this algorithm is to generate null lines, along which ReG or ImG equals zero. The intersection of these lines ($ReG = 0$ and $ImG = 0$) represents, to a better approximation than the initial guess, a zero of the complex function G . Assuming the function ReG is locally linear, this function should have a null point on exactly two or none of the rectangle’s sides. For each iteration, the function G is evaluated at each of the rectangle’s corners. Null points for ReG occur on sides bounded by corners for which the ReG evaluates to opposite signs. The unknown coordinate of the null point along a particular side is determined by linearly interpolating ReG between the two corners. The null line is then determined by connecting the two null points for ReG . An identical procedure for generating null points and a null line is performed for the function ImG . If, for either ReG or ImG , no null points are located, the iteration is repeated using a larger rectangle.

When an intersection point is determined, G is evaluated at that point. The algorithm ends when both $\text{Re}G$ and $\text{Im}G$ at the intersection point fall below a null criterion (typically 1 part in 10^{11}) specified by the user. This final intersection point is the final value for complex permittivity of the sample. If G remains larger than the null criterion, a new smaller rectangle is formed around the intersection point (see smaller rectangle in Fig. 1), and the null line intersection determination is repeated.

IV. Application of Technique to Future Experiments

A. Determining Permittivity of Non-Magnetic Liquid Samples (*Cassini*)

The simplest experiment to determine the permittivity of cryogenic hydrocarbon mixtures relevant to the *Cassini* science missions involves a three-region cylindrical cavity. Three separate resonant frequency sweeps using a vector network analyzer are performed, each with a different configuration of materials. The first sweep (Figure 2.a) is performed on an empty cavity to gain parameters necessary for computing wall losses. The second sweep (Figure 2.b) is performed on a cylindrical cavity with only an annular non-magnetic quartz holder inserted (Region 2). Exact cavity perturbation is then used to compute the dielectric constant of the quartz. The third sweep (Figure 2.c) is performed on a cavity with both the cryogenic liquid sample (Region 1) and the annular quartz holder inserted. Region 3 consists of free space between the holder and the cavity walls. Exact cavity perturbation is then used to compute the dielectric constant of the sample.

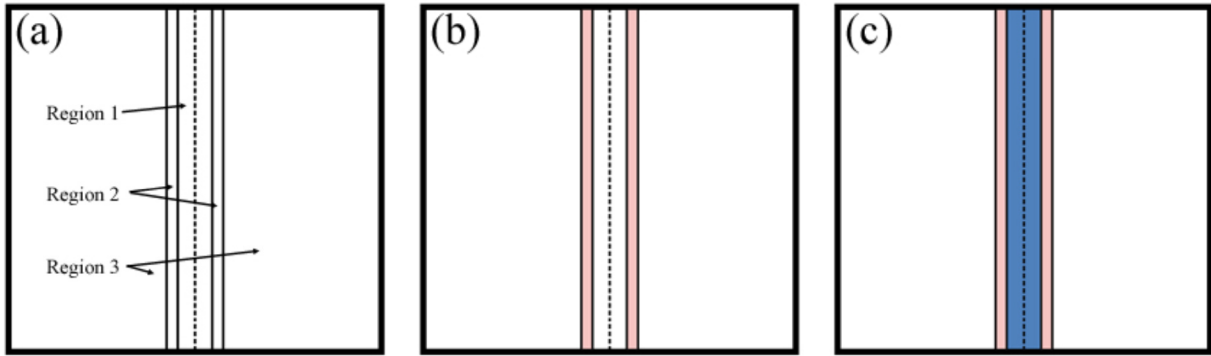


Figure 2. Schematics of cavity configurations for *Cassini* experiment

Assuming the sample and the holder are non-magnetic, power losses due to magnetic fields can be ignored. Regardless, arranging the sample close to the center of the cavity further validates this assumption because cavity magnetic fields vanish at this location.

B. Accommodation of Magnetic Samples

The exact cavity perturbation technique described in this paper is valid for non-magnetic samples. However, the technique can be easily extended to accommodate samples with both dielectric and magnetic properties. In defining the electric and magnetic fields equations used to compute the S matrix, a frequency-dependent propagation constant k_i is computed for each region within the cavity. In the technique described above, k_i is written as

$$k_i = 2\pi f \sqrt{(\epsilon_0 \cdot \epsilon_i) \cdot \mu_0},$$

where f is frequency and ϵ_i is the complex permittivity of the i^{th} region. The complex permeability of the i^{th} region (μ_i) is omitted, because $\mu_i = 1$ for non-magnetic samples. However, field equations can be modified for cavities loaded with magnetic samples simply by expressing k_i as

$$k_i = 2\pi f \sqrt{(\epsilon_0 \cdot \epsilon_i) \cdot (\mu_0 \cdot \mu_i)}.$$

In addition, the time-averaged energy storage expressions and power loss expressions used to compute quality factor must be adjusted to include magnetic contributions.

C. Iterative Technique to Simultaneously Compute Permittivity and Permeability

While it is possible to configure the cylindrical cavity to permit certain assumptions (i.e. positioning the sample at where the magnetic field vanishes so a relative permeability of one can be assumed), the four-sweep experiment proposed here allows both the permittivity and permeability to be obtained simultaneously. The first three sweeps (Figure 3.a-c) of this experiment are identical to the ones described in IV.A. Additionally, a fourth frequency sweep (Figure 3.d) is performed on a cavity configured such that the sample occupies a significantly larger percentage of the total cavity volume compared to the sample in the third sweep.

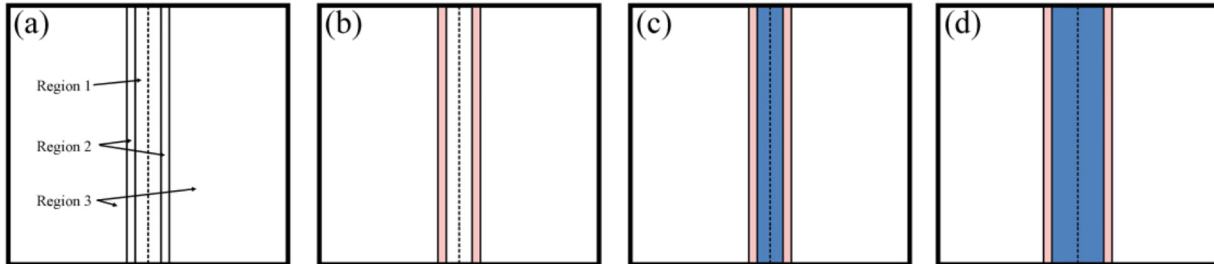


Figure 3. Schematics of cavity configurations for simultaneous permittivity/permeability determination

Like the experiment described in IV.A, the permittivity of the non-magnetic quartz holder (pink) is determined using exact cavity perturbation. Measurements from the first sweep can be related to wall losses. Now that the quartz holder permittivity is known, exact cavity perturbation is used to solve for the permittivity of the sample (blue), assuming its permeability is one (i.e. the sample is non-magnetic). This assumption, though approximately valid because the sample occupies only a small volume near the center of the cavity, is dealt with by performing exact cavity perturbation on measurements from the fourth sweep. Using the calculated value for sample permittivity from the third sweep, exact cavity perturbation is performed on measurements from the fourth sweep to determine the complex permeability of the sample.

Now that a first estimate of the permeability for the sample is known, a more accurate permittivity is computed using measurements from the third sweep, without having to assume the sample is non-magnetic. But because this adjusted permittivity value may not be equivalent to the one used to calculate permeability, the permeability computation using measurements from the fourth sweep is repeated. This process of repeating permittivity and permeability computations continues until neither value changes significantly from one iteration to the next. This process removes the third sweep assumption that the sample is non-magnetic because permittivity and permeability values have been found that satisfy measurements from both the third and fourth frequency sweeps. In practice, the experiment is simpler than described because most magnetic samples are solid and do not require a separate region for the quartz holder.

V. Acknowledgements

This research was carried out at the Jet Propulsion Laboratory, California Institute of Technology, and was sponsored by USRP and the National Aeronautics and Space Administration.

References

1. “Cassini: Spacecraft and Instruments” *NASA: Missions*, URL: www.nasa.gov/mission_pages/cassini/spacecraft [cited 6 May 2011].
2. Barmatz, M.B. and Jackson, H.W., Jet Propulsion Laboratory, Pasadena, CA, U.S. Patent Application for “New Technique for Performing Dielectric Property Measurements at Microwave Frequencies,” Docket No. CIT-5434, filed 8 September 2009.
3. Meng, B., Booske, J., and Cooper, R., “Extended Cavity Perturbation Technique to Determine Complex Permittivity of Dielectric Materials,” *IEEE Transactions on Microwave Theory and Techniques*, Vol. 43, No. 11, 1995, pp. 2633-2636.

4. Sphicopoulos, T., Bernier, L., and Gardiol, F., “Theoretical Basis for the Design of the Radially-Stratified Dielectric-Loaded Cavities Used in Miniaturised Atomic Frequency Standards,” *IEEE Proceedings*, Vol. 131, No. 2, 1984, pp. 94-98.
5. Pozar, D.M., *Microwave Engineering*, 3rd ed., John Wiley and Sons, Hoboken, 2005, Chapter 6.
6. Jackson, H.W. *Microwaves in a Loaded Cylindrical Cavity: Summary of Results*. Notes. November 13, 1992.
7. Jackson, H.W. *Direct Calculation of Stored Energy, End Plate Absorption and Q for a TM_{010} Mode in a Cylindrical Microwave Cavity Containing a Cylindrical Sample*. Notes. 14 February 1995.